ICP 2023 INTERNATIONAL CONFERENCE ON POLYGENERATION

Numerical Study of Polymer Embedded Metal Hydride-Based Self-Sensing Actuator

G Mohan, V Keshav

Center for Computational Research in Clean Energy Technologies, Sree Chitra Thirunal College of Engineering, Thiruvananthapuram, Kerala, India

Corresponding author E-mail address: mohan.g.menon@sctce.ac.in (G. Mohan)

Abstract

Metal hydride actuators have been gaining popularity over the last decade due to their attractive operational features like high power-to-weight ratio, noiseless and vibrationless operation, lightweight, safety and environmental benignancy. The studies on actuation caused by the mechanical expansion and contraction during sorption are scarce and mostly restricted to bimorph and unimorph actuators. Their stroke and force characteristics are limited to mostly micro-actuation only. A study using spring actuator driven by volume expansion of $LaNi_5$ alloy granular bed has previously been reported. Although a convenient alloy having desirable hydrogenation properties for miscellaneous applications, $LaNi_5$ undergoes frequent pulverization during sorption cycles owing to its brittleness and the large intrinsic strain induced by cyclic swelling and shrinkage. This incurs issues like reduced thermal conductivity and local stress concentrations at regions of the confinement where the pulverized powder densifies. To enhance their stability, polymer embedding is done. The main objective of this study is to conduct the performance simulation of metal-hydride based spring type actuator with polymer treatment and to compare it with that of granular bed. Parametric studies are done to comprehend the effects of salient operational and geometric parameters on the actuation behaviour. The simulation study is done using COMSOL Multiphysics commercial code. The results show that the composite bed renders better actuation performance than the granular bed in addition to reduction of decrepitation of the alloy. The thermal conduction in the composite bed is also found to be better relative to the powder bed due to which the former shows a quicker response. The parametric studies show the possibility for further optimization of the geometric and operational parameters.

Keywords: Actuator, Metal Hydride, $LaNi_5$

1. Introduction

Global warming is a significant problem which is responsible for climate change and other natural disasters that we have been facing since the last decade or so. ‘A low carbon economy’ is identified as the means to abate the greenhouse gas emissions contributing to global temperature rise. Hydrogen is a promising expedient for attaining industrial decarbonization. However, like electricity, hydrogen is an energy carrier, and a hydrogen economy aims to tap this energy for possible alternates to many existing conventional systems and processes that are essential contributors to the carbon footprint.

Metal hydrides are materials having great significance for a hydrogen-based economy. Although popular as a storage medium for hydrogen, they have wide scope for many practical applications. Metal hydride has the potential to exploit low quality heat which is a vital aspect in raising the reliability on renewables. With the advent of a prospective hydrogen economy, it is imperative to identify and explore different tools and methods to maximise the reliabilty on hydrogen. Hydride based actuation is one such key area that has enough room for investigation. Numerous studies have been carried out on hydrogen gas pressure driven actuators, primarily in rehabilitative systems and biomimetic systems like artificial muscles for instance [1,2,3]. The inherent property of metal hydrides to expand in volume during hydrogen charging process is intense enough to dispense an actuation force. The studies on such actuation caused by the mechanical expansion and contraction during sorption are scarce and mostly restricted to bimorph and unimorph actuators.

The manuscript revised as suggested.

Nomenclature

C_a&C_d	Material dependent constants	F	Reacted fraction
E_a&E_d	Activation energy	n	Phani-Niyogi exponent
A&B	van't Hoff constants	P_{eq}	Equilibrium pressure
E	Youngs modulus	P	Bed pressure
V	Volume fraction	T	Bed temperature
R	Universal gas constant	$\dot{m}$	Rate of change of H_2
D_f	Diffusivity	C_P	Specific heat
Nu	Nusselt number	Gr	Grashof number
Ra	Rayleigh number	Pr	Prandtl number
D	Coil diameter	d_0	Tube outer diameter
P_t	Axial pitch	L	Length of tube
h	Convective heat transfer coefficient	K_B	Boltzmann constant
H_a	Activation energy		
Greek letters			
P	Density	α	Thermal expansion coefficient
ϕ	Expansion ratio	μ	Dynamic viscosity
λ	Thermal conductivity	ß	Volume expansion coefficient
ε	Bed porosity	Ψ_{max}	Maximum filler volume fraction
ΔH	Enthalpy of formation	ΔS	Entropy of formation
Subscripts			
eq	Equilibrium	g	Gas
e	Effective value	p	Particle
b	Metal hydride bed	a	Absorption
0	Initial value	d	Desorption
sat	Saturated	f	Ambient fluid
q	Net value	cr	Critical value
c	Composite	m	Matrix

Y. Nishi *et* al. [4] studied the behaviour of a soft bimorph actuator comprising of two rubber sheets, one dispersed with $LaNi_3Co_2$ powder. Strains of 4000ppm is induced causing a large bending motion during hydrogenation from 100s to 10,800s. M. Mizumoto *et* al. [5] investigated the bending behaviour of Cu-plated hydrogen storage alloy. Plating of a non-hydrogenating element on hydrogenating element is done to convert the volume expansion of the latter to bending motion. They studied the displacement and response attributes for varying thickness of the hydride element and non-hydride element. Compared to 40μm hydride strip, for which the displacement at the top end in the horizontal sense is 7.5mm at 6min, for 20μm thickness situation, improved displacement and response time values respectively of 21mm and 1min were obtained. K. Goto *et* al. [6] studied the deformation in a capsule-type metal hydride actuator. The actuator consists of a hollow epoxy resin capsule with a metal hydride foil placed partially in its inner wall. The expansion of hydride foil during hydrogen absorption will force the contraction of capsule. A piston can be mount on the capsule to attain a linear actuation. The maximum displacement obtained is 14μm.

The general problems of these actuators include their slow response speeds and low force-stroke characteristics. The chief governing factor for actuation is hydrogen sorption, which is controlled by heat transfer from the bed. Adapting mechanisms or structural modifications that can augment its heat transfer rates will aid in improving the sorption rates and in turn the overall performance of these actuators. The selection of a suitable geometry that could manipulate the elastic potential on its walls for an appreciable actuation due to expansion or contraction of metal hydride, is important. A study using spring actuator driven by volume expansion of $LaNi_5$ hydriding alloy granular bed has previously been reported [7]. Such actuators can be utilized for remote sensing and actuation providing response

to thermal/pressure stimuli. The cyclic stability of the granular bed is a matter of concern as it can culminate in issues like stress concentration, reduced thermal conductivity and hindered actuation performance. During cyclic sorption, the alloy particles get refined resulting in reduced particle surface and contact that lead to heat accumulation. This phenomenon can ultimately cause the powder to solidify after subsequent expansion-contraction cycles. For remote sensing /actuation applications demanding larger working cycles, this would be an inconvenience. Polymer mixing of hydride is done with an intend to alter its decrepitation during sorption cycles. Polymers being poor conductors of heat should be altering the overall heat conduction, but by providing a better path for the heat front to travel relative to the point contact between powder particles, we could actually enhance the heat conductivity. This work is a novel attempt to tailor the prospects of polymer treatment of metal hydride alloy with a convenient geometry for an actuator application.

The main objective of this work is to investigate the actuation performance of such an actuator having $LaNi_5$-polymer composite bed and to juxtapose it with a granular bed arrangement both in spring-type enclosures. In the present study numerical simulations are performed on coiled self-sensing actuator filled with polymer-embedded $LaNi_5$ alloy. Effect of salient geometric and operating parameters on its performance is also investigated.

2. Methodology

The physical model of the coiled tube bed is shown in Fig. 1. The geometric parameters of the coiled tube for both granular bed and composite bed are given in Table 1. It must be noted that for the accommodation of same mass of $LaNi_5$ as in granular bed, the volume required for the composite bed is more. This is realized by taking 8.32 turns for the composite coiled tube bed compared to 5 turns for the powder bed. 100 mm is the minimum coil diameter required to coil a AISI 316 tube with a maximum wall thickness of 1.65 mm, to the suitable no. of turns, without any distortions. For the composite bed, the wall thickness may not necessarily be 1.65 mm. This maximum limit is usually considered to withstand the large stress induced by the powder bed, especially at higher denser regions that are formed by alloy pulverization. This is not a requisite for polymer embedded hydride bed.

Table 1: Geometrical parameters used for the simulation of granular bed ($LaNi_5$ powder bed) and composite bed ($LaNi_5$-Si bed)

	$LaNi_5$ powder bed	$LaNi_5$-Si bed
No. of coils	5	8.32
Stainless- steel tube diameter	12.7 mm	12.7 mm
Stainless- steel tube thickness	1.65 mm	1.65 mm
Hydride bed thickness	3 mm	3 mm
Hydrogen filter diameter	3 mm	3 mm
Axial pitch of the spring arrangement	36 mm	36 mm
Mean diameter of the spring	100 mm	100 mm
Total weight of hydride	0.4056 kg	0.4056 kg

The polymer matrix resists the alloy break down, densification and agglomerations. It also alters the thermal conduction resistance between adjacent particles. One issue however is the negation of volume expansion effect for actuation by the elastic deformation of the polymer matrix. This can remarkably reduce the expansion effects depending upon the volume of dispersant and rubber matrix [8]. Hence based on the critical value in terms of the net incompressible expansion of particulate dispersed polymer composite, thinner walled tubes can be considered. This offers less resistance and better actuation for the polymer applied case. However, for relevant comparisons, same thickness of the tube is accounted in each case.

The geometry is tested to sustain a pressure within yield equivalent to 2.5 times the maximum working pressure. This is conforming to [7] which says that the volume swelling of the hydride bed is 2.5 times hydrogen gas pressure during hydrogen formation. Heat transfer with air by free convection is considered. A suitable heat flux is assigned accordingly. To make the simulation less complex, relevant assumptions are made:

- The polymer-hydride composite is isotropic.
- The hydriding alloy considered is having negligible plateau slope and hysteresis.
- The association of the hydride and polymer does not alter the hydrogen storage capacity of the alloy.
- The dispersed alloy particles are spherical.
- The pressure drop across the bed thickness is negligible.
- The gas diffusion resistance offered by the polymer is neglected.
- Convection and conduction are the predominant heat transfer modes and radiation effects are negligible.
- The inertial effects of the spring are neglected.

2.1 Problem formulation

Mass balance: Hydrogen gas is supplied to the bed through the porous filter. The mass transport of hydrogen within the hydride bed driven by concentration gradient is represented using the following equation:

$$(1-\varepsilon)\frac{\partial \rho_b}{\partial t} = \dot{m} + (1-\varepsilon)\frac{\partial}{\partial x}\left(D_f \frac{\partial \rho_b}{\partial x}\right) + (1-\varepsilon)\frac{\partial}{\partial y}\left(D_f \frac{\partial \rho_b}{\partial y}\right) \quad \text{(Eq.1)}$$

LHS gives the rate of change of mass of the hydride bed. The first term in RHS gives the mass flow rate of hydrogen gas and the second and third terms represents the diffusive transport due to concentration gradient in the bed.The potential of the gas to diffuse into the sorbent medium is given using the diffusivity relation.

$$D_f = D_{f_0} \exp\left(\frac{-H_a}{K_B T}\right) \quad \text{(Eq.2)}$$

Energy balance: Depending on whether the process is absorption or desorption, heat gets released or absorbed. Heat conduction transport across the hydride bed is represented using the equation:

$$(\rho C_P)_e \frac{\partial T}{\partial x} = \lambda_e \left[\frac{\partial}{\partial x}\left(\frac{\partial T}{\partial x}\right) + \frac{\partial}{\partial y}\left(\frac{\partial T}{\partial y}\right)\right] - \dot{m}\Delta H \quad \text{(Eq.3)}$$

The first term in the LHS accounts the heat conducted across the bed and the second term represents the heat absorbed or desorbed by the bed respectively during dehydrogenation and hydrogenation. The polymer embedded with hydride alloy is a case of particle dispersed composite with the metal hydride being the dispersed particles. For convenience and to avoid the complex formulations, the hydride particles are assumed to be spherical. Among the classical models, the Lewis-Nielsen model gives appreciable results for the effective thermal conductivity of particle dispersed composites with moderate filler fractions up to 40% [10].

$$\frac{\lambda c}{\lambda m} = \frac{1+QWVp}{1-W\varphi Vp} \quad W = \frac{\frac{\lambda}{\lambda_m}-1}{\frac{\lambda}{\lambda_m}+Q} \quad \varphi = 1 + \left(\frac{1-\Psi_{max}}{{\Psi_{max}}^2}\right) V_P \quad Q = 1.5 \text{ for spherical particles} \quad \text{(Eq.4)}$$

Reaction kinetics: The sorption kinetics equations are given as follows:

$$Absorption\ rate:\ \dot{m} = C_a \exp\left(\frac{-E_a}{RT}\right) \ln\left(\frac{P}{Peq}\right) \cdot (\rho_{sat} - \rho_b) \quad \text{(Eq.5)}$$

$$Desorption\ rate:\ \dot{m} = C_d \exp\left(\frac{-E_d}{RT}\right) \ln\left(\frac{P-Peq}{Peq}\right) \cdot (\rho_b) \quad \text{(Eq.6)}$$

These are semi-empirical relations that govern the absorption and desorption of metal-hydride. The equilibrium pressure is determined as from van't Hoff plot:

$$\ln P_{eq} = A - \frac{B}{T} \quad \text{(Eq.7)}$$

This equation controls the behaviour of the hydride at the plateau region. A hydrogen gas supply pressure above this pressure starts hydrogenation and when the supply pressure is below this value, dehydrogenation occurs.

Variation in porosity: The change in porosity of the reactor bed due to bed particle expansion and contraction is given by [11]:

$$\varepsilon = 1 - (1 - \varepsilon_0)\frac{1+\phi_p F}{1+\phi_b} \qquad \text{(Eq.8)}$$

Porosity input is a record of the packing rate or the mass of the metal assembled in a bed. The variation in porosity during hydriding/dehydriding process is minor and their effect on the bed properties is insignificant. During sorption, the particles bulge out or shrink making differential area contact eventually causing slight modifications to the bed thermal conductivity and heat capacity.

Convective heat transfer coefficient: For vertical helicoid tube, the convective heat transfer coefficient is obtained from the set of relations given in [12]. For natural convection, the fluid molecules that get heated, due to their relative low density rises up and the low temperature molecules descend. Density variation is therefore the driving force for free convection. From the following expressions, the convective heat transfer coefficient can be determined.

$$H = \frac{Nu\lambda}{d_0} \qquad Nu = 0.0779(Ra)^{0.275}\left(\frac{D}{do}\right)^{0.184}\left(\frac{P_t}{do}\right)^{0.212}\left(\frac{L}{do}\right)^{0.108} \qquad \text{(Eq.9)}$$

$$Gr = \frac{\rho^2 \beta g \Delta T L^3}{\mu^2} \quad Pr = \frac{C_P \mu}{\lambda} \quad Ra = GrPr$$

Structural mechanics equations

Properties of $LaNi_5$ is taken as the properties for the particle and that of Silicone rubber is considered for properties of the matrix in the empirical relations used to determine the effective values of the composite bed.

Effective Youngs modulus: Considering the effect of bed porosity, the effective elastic modulus is given by Phani-Niyogi equation [13]:

$$E_e = E_q\left(1 - \frac{\varepsilon}{\varepsilon_{cr}}\right)^n \qquad \text{(Eq.10)}$$

Here, ε_{cr} is the critical porosity at which the neighbouring particles does not make any contact. The net mechanical properties of a two-phase composite can be obtained from the law of mixtures which considers that each component phases contribute to the effective property regarding their volume fractions. This model assumes that mixture constituents experience the same strain.

$$E_q = E_p V_p + E_m V_m \qquad \text{(Eq.11)}$$

Expansion coefficient: The following relation gives the coefficient of expansion of the hydride bed accounting both thermal and volumetric expansion of the hydride, that vary linearly with bed temperature [14].

$$\alpha_e = \alpha\left[1 + \alpha\Delta T + \frac{\phi_b}{3\alpha\Delta T} F\right] \qquad \text{(Eq.12)}$$

The factors governing the coefficient of thermal expansion of a particle dispersed composite are the particle shape, size, distribution, and volume fraction, and also the interfacial characteristics of the matrix and dispersion or between the dispersed particles for the case of higher particular concentrations. Turner's modification [15] to Voigt model gives the effective thermal expansion for composites as follows:

$$\alpha = \frac{V_p E_p \alpha_p + V_m E_m \alpha_m}{V_p E_p + V_m E_m} \qquad \text{(Eq.13)}$$

Initial and boundary condition: The initial temperature and pressure of spring bed is assumed to be a constant.

$$\rho_{b_0} = \rho_b; \qquad P = P_0; \qquad T = T_0 \qquad \text{(Eq.14)}$$

The entire spring bed is leakage proof and hydrogen gas is supplied at a constant pressure to the reactor bed. The heat transfer to and from the spring bed manifests through the heat flux at the outer surface of the spring walls. The heat transfer coefficient consideration is based on free convection. Hydrogen is supplied through a porous filter insert concentric to the spring bed. Therefore, the boundary

between the bed and the filter tube is permeable to hydrogen gas transfer as well as heat transfer. The boundary conditions are therefore as follows:

- *At the spring wall*:
$$\partial\rho = 0; \qquad \partial P = 0; \qquad -\lambda_e \partial T = h_f(T_f - T) \text{ at } t > 0 \qquad \text{(Eq.15)}$$
- *At the porous filter tube wall:*
$$\partial\rho_b = 0; \qquad P = P_0; \qquad \partial T = h_g(T_g - T) \text{ at } t > 0 \qquad \text{(Eq.16)}$$
- The base end of the spring is fixed, and the spring is constrained to undergo motion only in the axial direction.

2.2 Simulation methodology

The simulation study is done using COMSOL Multiphysics 6.0.0.318. The initial study is done on hydride powder bed followed by hydride-polymer alloy bed. Three application modules are used for the simulation study. 'Transport of dilute species in porous media' is used to simulate the sorption process in the hydride bed. 'Heat transfer in porous media' is used to simulate the heat transfer due to convection at the outside interface of the coiled tube, the conduction of heat between the tube and the bed, and the heat transport within the granular bed. 'Solid mechanics' module is used to simulate the structural mechanics of the system like thermal expansion, volume expansion, force, and stroke. Material properties for AISI 316, Hydrogen gas and Silicone rubber are obtained from literature [7] [14] [16]. Boundary and initial conditions are provided as necessary. The entire geometry considering the essential physics modules are discretized into tetrahedral and prism elements.

The validation of the adopted physics modules was done with reference to the experimental studies done in [8]. Si rubber and $LaNi_5$ mixed in the ratio of 40/1 weight ratio, is coated over a brass tube which is subsequently sealed in a larger tube. Heat transfer is assured by flowing water through the brass tube. Hydrogen gas is supplied to the concentric tube enclosing the coated brass tube and the hydrogen sorption process in the coating is studied. The schematic of the setup is given in Fig. 2. An average deviation of 5.54% is observed.

3. Results and discussion

3.1 Comparison of simulation results of granular and composite bed

The hydride alloy used for the simulation study on spring actuator is $LaNi_5$. With regard to the choice of polymer, a couple of works have been reported on $LaNi_5$ embedded in Si rubber [8,17]. These studies do not imply the impediment of the maximum hydrogen storage capacity of the alloy, however points out the slower kinetics and larger effort requirement for the activation of hydride within the polymer matrix. This is due to the gas barrier behaviour of rubber matrix. The initiation of structural defects due to fatigue cycles actually reduces the resistance offered by the polymer to gas permeation through the nucleation of hydrogen transport paths. Nonetheless the polymer matrix properly serves its purpose of imparting better structural stability to the hydriding alloy and other additional perks like oxidation resistance, better heat transport part and appreciable gravimetric storage capacity [18][8] relative to untreated alloy powder bed.

The large volume differences in the metal and hydride phase develops a remarkable intrinsic strain within the particle lattice leading to its decrepitation. As the particles break down within the granular media numerous issues can take shape- reduced effective thermal conductivity within the bed due to very small contact area between neighbouring particles, localized densifying which develops localized stress concentrations in further cycling process, agglomeration of the refined particles due to increased friction and cohesion, and so on. Additionally, loading of coiled tube with the alloy powder inclusive of the porous hydrogen supply pipe has very less feasibility too. To overcome these complications, the reliability of hydride alloy-polymer mixture for spring type actuator has been investigated. Owing to their high tensile strength and resistance to hydrogen embrittlement, AISI 316 material is considered for the coiled tube enclosure. The basic physical properties of $LaNi_5$, Si rubber and AISI 316 is given in Table 4.1. The initial values for various parameters used for the simulation are given in Table 3.

The comparison of the coiled tube bed temperature, concentration and resultant stroke during hydrogenation is shown in Figure 3. $LaNi_5$ considered for the simulation amounts to 84 wt.% in the polymer-hydride composite. This would render an effect similar to particle dominant composite as

studied in [19]. For this case the alterations in the hydrogen dissolution capacity of the hydride due to polymer association can be neglected and the polymer serves as a binder only. From Fig. 3 it is evident that the heat transfer rates in the composite bed is more significant compared to the powder bed. The main reason for this behaviour of the composite bed is the relatively lower thermal conductive resistance compared to the granular bed. The absorption rate for the composite bed is hence quicker than the granular bed. This is due to the better heat transfer within the bed and between the walls and bed. The contribution of convective heat transfer is maintained constant in both cases to account the changes in conduction properties alone which are direct implications of using two distinct structural media for the bed.

Table 2: Physical properties of $LaNi_5$, Si rubber & AISI 316 used for simulation ([7],[14],[16])

	$LaNi_5$	**Hydrogen**	**AISI 316**	**Si rubber**
Activation energy for absorption (Ea) [$Jmol^{-1}$]	21170	-	-	-
Specific heat (Cp) [$Jkg^{-1}K^{-1}$]	419	14.890	468	1050
Density [kgm^{-3}]	8200	0.0838	8000	1100
Reaction kinetics constant (Ca) [s^{-1}]	59.187	-	-	-
Van't Hoff constant (A)	12.99	-	-	-
Van't Hoff constant (B)	3704.59	-	-	-
Thermal conductivity [W/ m.K]	20	0.1825	13.6	0.2
Thermal expansion coefficient [$mm^{-1}K^{-1}$]	1.23e-5	-	1.8e-5	250e-6
Modulus of elasticity [GPa]	140	-	204	0.001
Poisson's ratio	0.31	-	0.3	0.47

Table 3. Parametric ranges used in the simulation

	Absorption	**Desorption**
Constant bed pressure (bar)	5	1
Initial bed temperature (K)	295	330
Initial bed concentration (mol/m^3)	18981.48	19228.24
Heat flux temperature (K)	295	330
Convective heat transfer coefficient (W/m^2K)	22-27	22-27
Effective thermal conductivity of granular bed (W/mK)	0.75	0.75
Effective thermal conductivity of composite bed (W/mK)	0.3993	0.3993

Certain non-linear instances observed in the displacement curve of the composite is due to the influence of thermal contraction of rubber. Si rubber has a high thermal expansivity relative to the metal alloy. The non-linearities observed in the stroke plot is parallel to temperature variations in the bed and therefore this can be identified as the reason for the corresponding behaviour. For both cases. the initial absorption is governed by the material properties and is rapid. This is represented by the initial slope of concentration plot during hydrogenation. Rest of the process is governed by heat transfer in bed. After saturation, no more heat gets rejected from the bed and the heat flux effect kicks in, reducing the bed

temperature. The stroke and force characteristics of the granular bed is shown in Fig. 4 (a) and 3 (c) respectively. The maximum stroke is approximately 5.84 mm. Apparently hydride swelling is the significant contributor to actuation stroke although hydrogen gas pressure and thermal expansion of the bed chip in as well, but on a relatively small scale. To estimate the actuation force, the spring was subjected to boundary loads in the range of 0-60 N and the boundary load corresponding to which the actuation stroke gets completely negated is deemed as the required force value. The actuation force is therefore approximated as 60N for powder bed case.

A maximum stroke of approximately 12 mm is observed for the composite bed. For this case also, hydride expansion is observed to be the primary source for relevant actuation. The actuation force is also evaluated in a similar way as done for the granular bed. The force for complete neutralisation of the actuator stroke is observed to be approximately 100 N. For both the cases, an initial stroke of 1 mm within 10-15s is observed. This is pertaining to the sorption process undergone by the influence of material properties of the hydriding alloy.

3.2 Effect of operational parameters on hydrogenation

The absorption rate increases with H_2 gas pressure. The response to maximum stroke therefore increases with supply pressure of hydrogen. The pressure differential between the hydrogen gas pressure and bed equilibrium pressure is the driving force for sorption process. So, for a constant temperature bed, when hydrogen gas pressure increases, the rate of hydrogenation/dehydrogenation increases. This effect for the composite and granular beds during hydriding process are shown in Fig. 5 and Fig. 9 respectively.

With increase in convective heat transfer coefficient the sorption rate is observed to increase. Quicker the heat transfer rates, the hydrogenation process will be completed quickly. Since volume swelling of the hydriding bed is a function of hydrogen sorption, the actuator displaces to its maximum stroke in a shorter time. The influence of heat transfer coefficient in improving the sorption rate and actuator response during hydrogen absorption is shown in Fig. 6 and Fig. 10 respectively.

For larger bed thickness, the heat conduction rates are less and the hydrogen absorption process takes longer time to complete relative to lower bed thickness condition. However, owing to larger actuation forces exerted by the larger hydride volume, the actuation stroke is observed to increase with be thickness. This result for the powder bed and the composite bed during hydrogen absorption process is shown in Fig. 7 and Fig. 11 respectively.

In any case, the change in temperature of the bed is proportional to the increase or decrease of hydrogen concentration in the bed. This complies with the endothermic-exothermic nature of sorption process. The semblance in the stroke and concentration graphs shows the predominant dependency of the former on the latter.

3.3 Effect of spring geometrical parameters on hydrogenation

With increment in spring pitch, the stroke gets raised. When the axial pitch increases for a given wire diameter, the shear strength of the spring decreases, resulting in larger actuation stroke. The effect of axial pitch of the spring type hydride-based actuator on the maximum stroke for powder bed case and composite bed case during hydriding process is shown in Fig. 8 (a) and Fig. 12 (a) respectively.

As the coil diameter increases, the spring stroke gets altered. For a coiled tube having a certain hydride storage capacity, the axial deflection of the coil decreases with increase in coil diameter. This is due to increase in shear strength imparting more strength to the geometry. Fig. 8 (b) and Fig. 12 (b) gives the variation in axial displacement of the spring for different coil diameters, for the granular and composite beds respectively.

4. Conclusions

The main intend behind using a polymer embedded metal hydride is to impart better resistance to decrepitation of the alloy due to cyclic expansion and shrinkage that would otherwise result in low bed thermal conductivity. The actuation force for the composite bed is 100N with a maximum stroke of 12mm compared to 60N and 5.84mm respectively for the powdered bed. The better actuation performance is an added advantage to the purpose of choice for polymer treatment. From the parallelism in the trends of the concentration and displacement variations for either case, it can be concluded that sorption driven volume expansion is the main contributor to actuation. The initial quick response in the

general sense, although in the millimeter scale, can be used as a marker for various sensing parameters. For improving the overall response rates of the actuators, the heat transfer rates from the bed must be augmented. The actuation force can be increased by considering thicker beds. It is also possible to get different stroke -force instances for different coil pitch and diameter. On the grounds of better heat transfer rates, we can conclude that the polymer metal hydride composite bed is better suited for the studied actuation application than its granular form. Heat transfer enhancement methods can be vital to the performance enhancement of these devices.

REFERENCES

[1] George M. Lloyd and Kwang J. Kim, Smart hydrogen/metal hydride actuator, *International Journal of Hydrogen Energy 32*, (2007) 247-255

[2] Kwangmok Jung and Kwang J. Kim, A Thermokinetically Driven Metal-Hydride Actuator, *Proceedings of SPIE, Vol.6932, Sensors and Smart Structures Technologies for Civil, Mechanical and Aerospace Systems*, (2008)

[3] Minako Hosono, Shuichi Ino, Mitsuru Sato, Kazuhiko Yamashita, Takashi Izumi, A System Utilizing Metal Hydride Actuators to Achieve Passive Motion of Toe Joints for Prevention of Pressure Ulcers: A Pilot Study, *Rehabilitation Research and Practice*, (2012)

[4] Yoshitake Nishi, Haruhisa Uchida, Hiromasa Yabe, Byungsuk Kim, Takashi Ogasawara, Giant Bending Motion of a Soft Actuator Controlled by Hydrogen Gas Pressure, *Journal of Intelligent Material Systems and Structures, Vol.17(8)*, (2006) 709-711

[5] Masayuki Mizumoto, Takeshi Ohgai, Akio Kagawa, Bending behavior of Cu-plated Pd-Ni alloy ribbon driven by hydrogenation, *Journal of Alloys and Compounds 482*, (2009) 416-419

[6] Kenta Goto, Tomoyuki Hirata, Takehiro Higuchi, Ohmi Fuchiwaki, Shingo Ozaki, Wataru Nakao, Deformation mechanism of capsule-type hydrogen-storage-alloy actuator, *International Journal of Hydrogen Energy 44*, (2019) 16877-16886

[7] P. V. Jithu, G. Mohan, Performance simulation of metal hydride based helical spring actuators during hydrogen sorption, *International Journal of Hydrogen Energy Vol.47, Issue 33I,* (2022) 14942-14951

[8] P. R. Bidez, A. J. Goudy, A. Zarynow, Hydriding and dehydriding kinetics of $LaNi_5$ mixed with Silicone Rubber, *Micromechanical Journal 47*, (1993) 108-114

[9] Fukai Y, The Metal-Hydrogen System, *Springer Series in Materials Science, Vol.2*, (1993)

[10] Karol Pietrak, Tomasz S. Wiśnieswski, A review of models for effective thermal conductivity of composite materials, *Journal of Power technologies 95(1)*, (2005) 14-24

[11] Chaker Briki, Patricia de Rango, Sihem Belkhiria, Mohamed Houcine Dhaou, Abdelmajid Jemni, Measurements of expansion of $LaNi_5$ compacted powder during hydrogen absorption/desorption cycles and their influences on the reactor wall, *International Journal of Hydrogen Energy, Vol.44, Issue 26*, (2019) 13647-13654

[12] M. Moawed, Experimental investigation of natural convection from vertical and horizontal helicoidal pipes in HVAC applications, *Energy Conversion and Management 46*, (2005) 2996-3013

[13] K. K. Phani, S. K. Niyogi, Youngs modulus of porous brittle solids, *Journal of Materials Science 22*, (1987) 257-263

[14] Lekshmi Dinachandran, G. Mohan, Numerical simulation of the parametric influence on the wall strain distribution of vertically placed metal hydride based hydrogen storage container, *International Journal of Hydrogen Energy, Vol. 40, Issue 16*, (2015) 5689-5700

[15] V. I. Borzenko. I. A. Romanov, D. O. Dunikov, A. N. Kazakov, Hydrogen sorption properties of metal hydride beds: Effect of internal stresses caused by reactor geometry, *International Journal of Hydrogen Energy 44*, (2019) 6086-6092

[16] AZoM.com- An AZoNetwork Site (2022)

[17] H. Uchida, T. Ebisawa, K. Terao, N. Hosoda, Y. C. Huang, Hydriding and Dehydriding Characteristics of $LaNi_5$ Mixed with Silicone Compounds, *Journal of the Less-Common Metals, 131*, (1987) 365-369

[18] Wayde R. Schmidt, Hydrogen storage in polymer-dispersed metal hydrides, *Proceedings of the 2001 DOE Htdrogen Program Review NREL/CP-570-30535*, (2001)

[19] R. Checchetto, N. Bazzanella, A. Miotello, G. Carotenuto, Synthesis and characterization of polymer embedded $LaNi_5$ composite material for hydrogen storage, *Journal of Physics D: Applied Physics 40*, (2007) 4043-4048

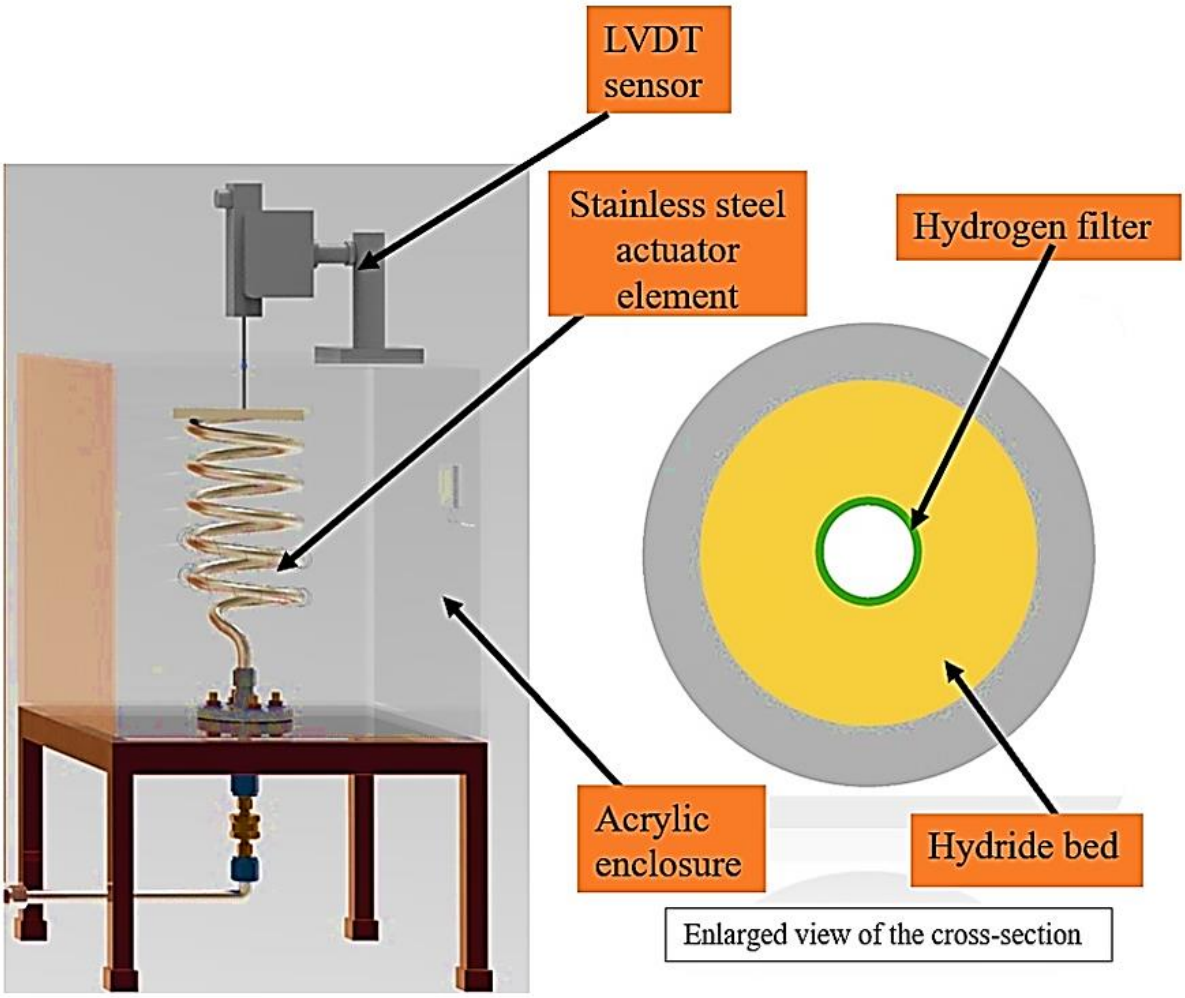

Figure 1: Schematic of metal hydride-based spring type actuator

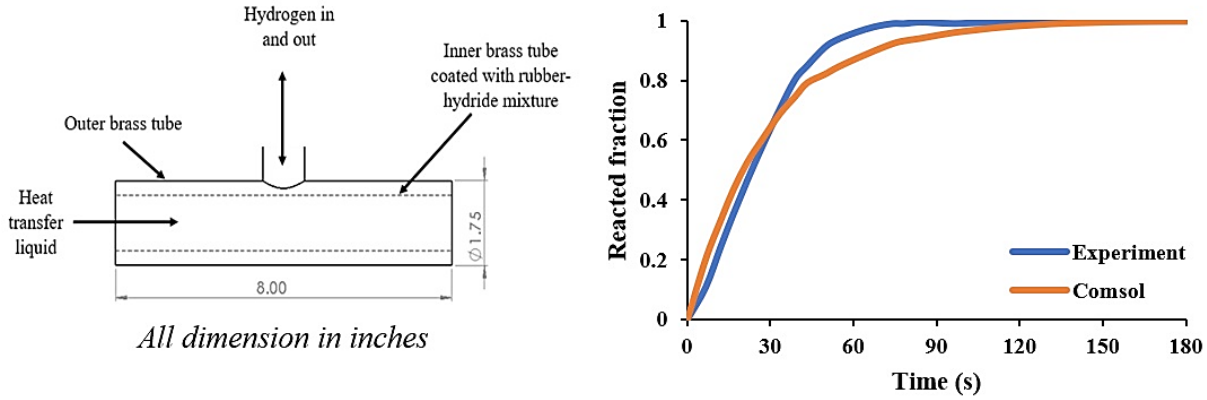

Figure 2**:** Schematic of experimental setup [8]

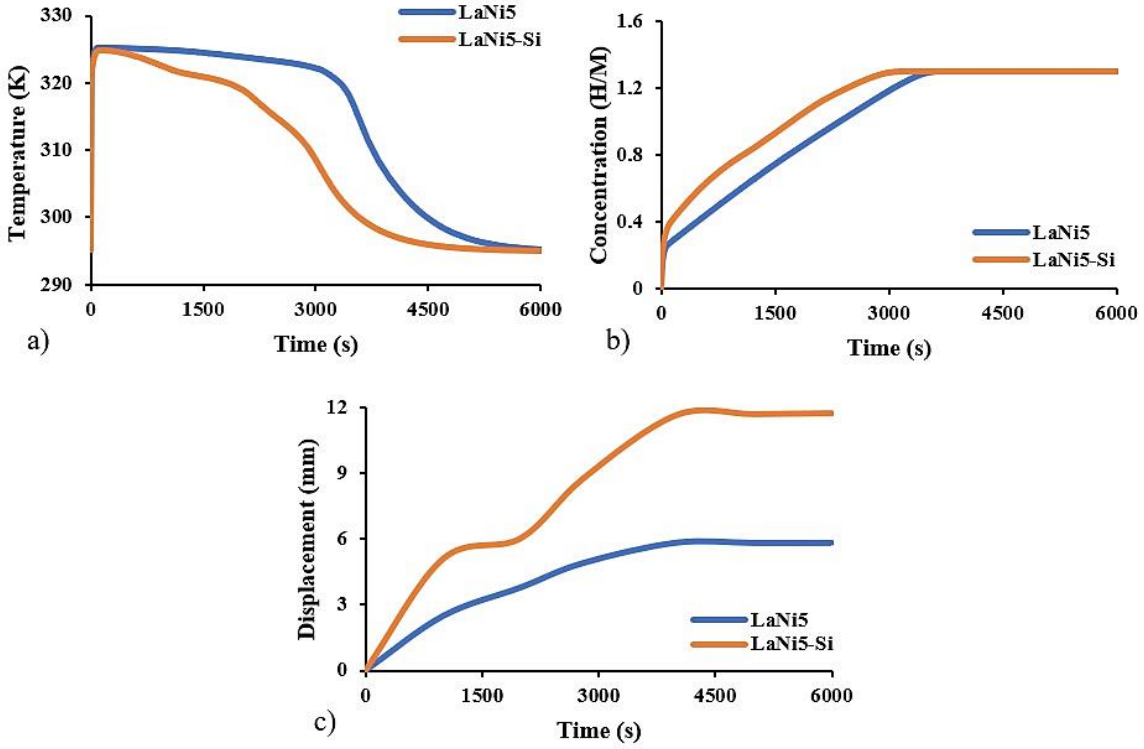

Figure 3: Comparison of variation of a) average bed temperature b) average bed concentration c) actuation stroke of hydride powder and composite beds (T_o =295K, P_o =5 bar, h=22W/m^{2}K, Bed thickness= 3 mm, Axial Pitch= 36mm, Spring constant= 7.874, Coils = 5($LaNi_5$) 8.32 ($LaNi_5$-Si))

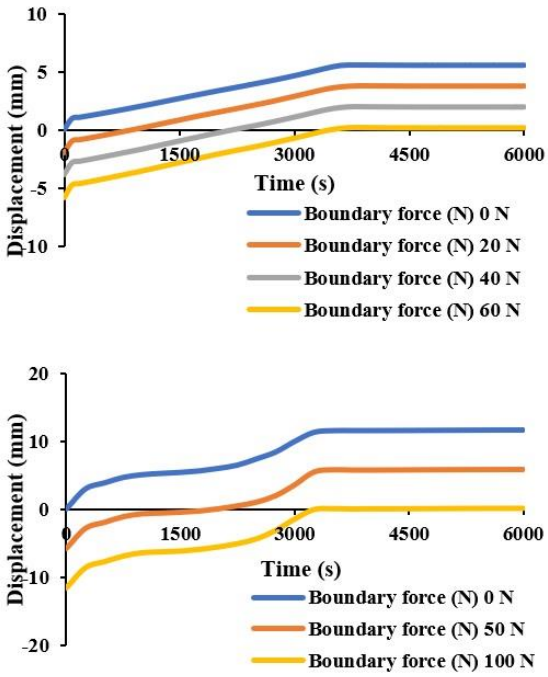

Figure 4: Comparison of actuator stroke in hydride powder and composite beds when subjected to different loads (T_o =295K, P_o =5 bar, h=22W/m^{2}K, Bed thickness= 3 mm, Axial Pitch= 36mm, Spring constant= 7.874, Coils = 5($LaNi_5$) 8.32 ($LaNi_5$-Si))

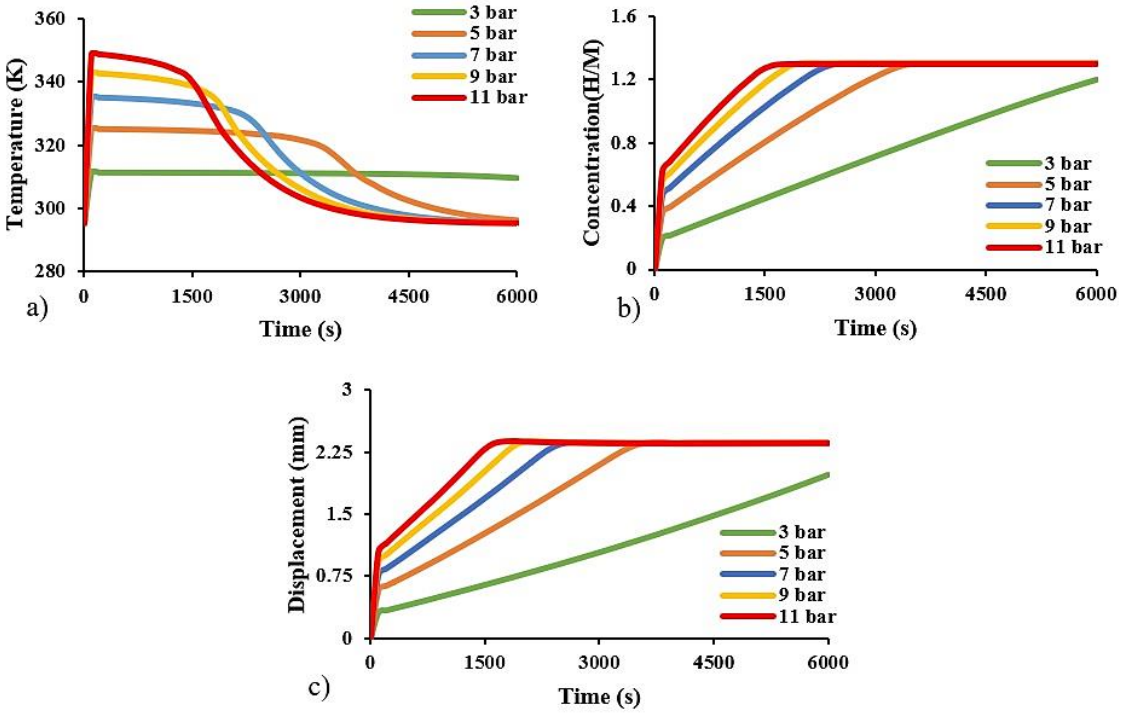

Figure 5: Effect of H_2 supply pressure on a) Average bed temperature b) Bed concentration c) Actuator displacement during hydriding process in granular bed (T_o =295K, P_o =3-9 bar, h=22W/m^{2}K, Bed thickness= 3 mm, Axial Pitch= 36mm, Spring constant= 7.874, Coils = 5($LaNi_5$) 8.32 ($LaNi_5$-Si))

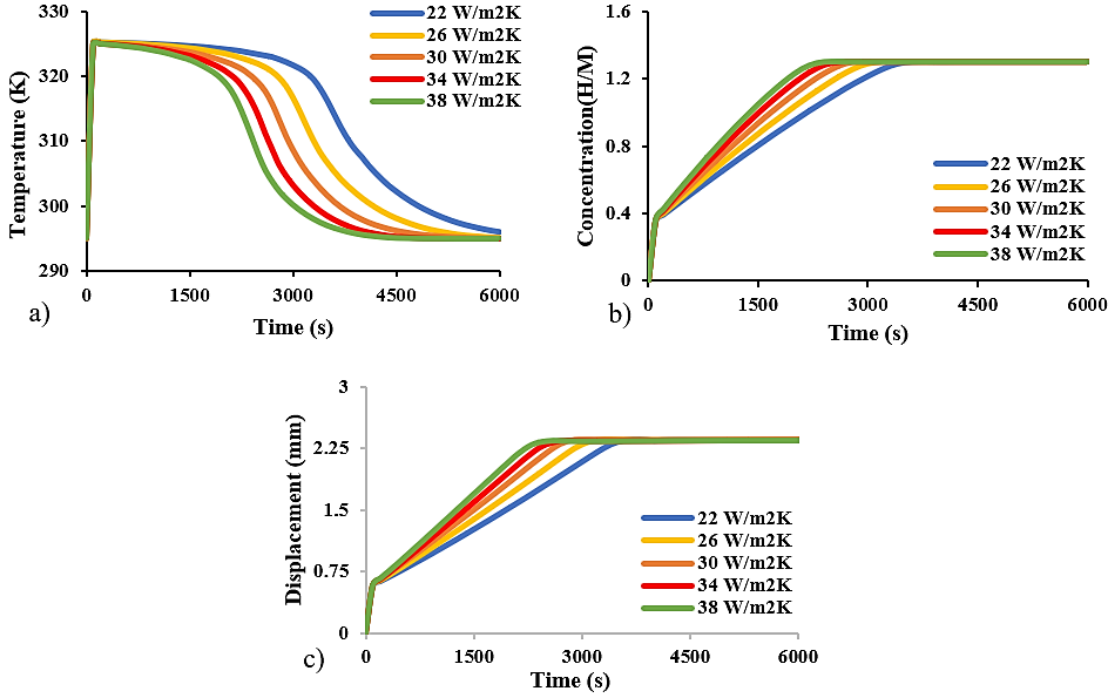

Figure 6: Effect of heat transfer coefficient on a) Average bed temperature b) Bed concentration c) Actuator displacement during hydriding process in granular bed (T_o =295K, P_o =5 bar, h=22-38W/m^{2}K, Bed thickness= 3 mm, Axial Pitch= 36mm, Spring constant= 7.874, Coils = 5($LaNi_5$) 8.32 ($LaNi_5$-Si))

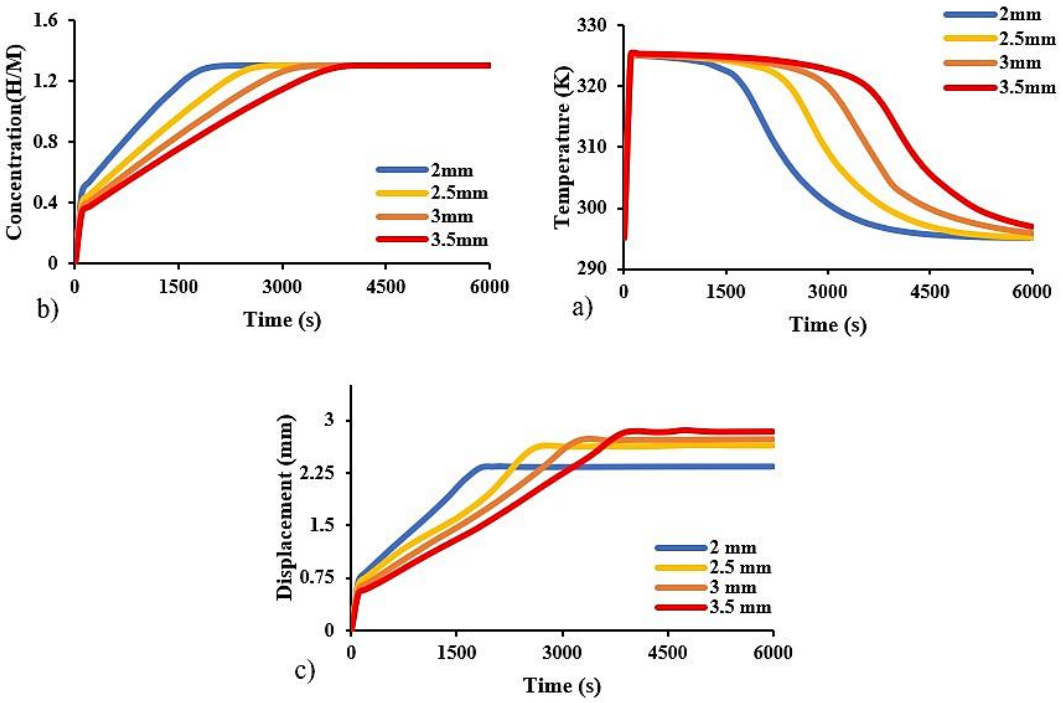

Figure 7: Effect of bed thickness on a) Average bed temperature b) Bed concentration c) Actuator displacement during hydriding process in granular bed (T_o =295K, P_o =5 bar, h=22W/m^{2}K, Bed thickness= 2-3.5 mm, Axial Pitch= 36mm, Spring constant= 7.874, Coils = 5($LaNi_5$) 8.32 ($LaNi_5$-Si))

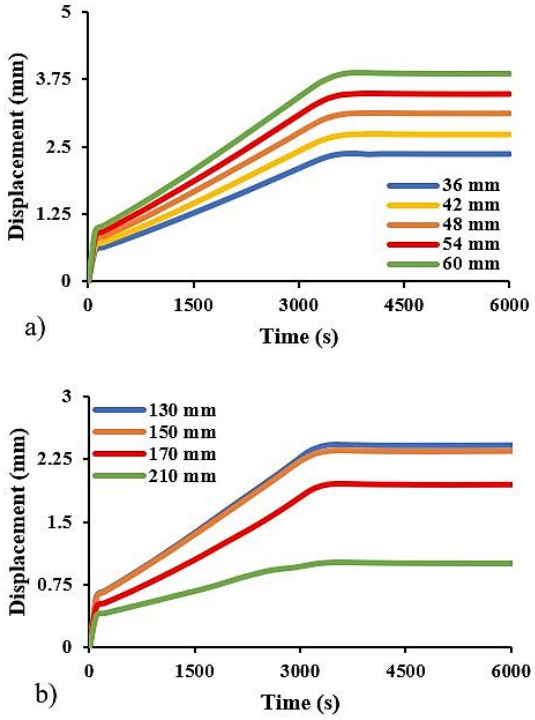

Figure 8: Effect of a) coil pitch and b) coil diameter on actuator displacement during hydriding process in granular bed (T_o =295K, P_o =5 bar, h=22W/m^{2}K, Bed thickness= 3 mm, Axial Pitch= 36-60 mm, Spring constant= 10.236-16.535, Coils = 5($LaNi_5$) 8.32 ($LaNi_5$-Si))

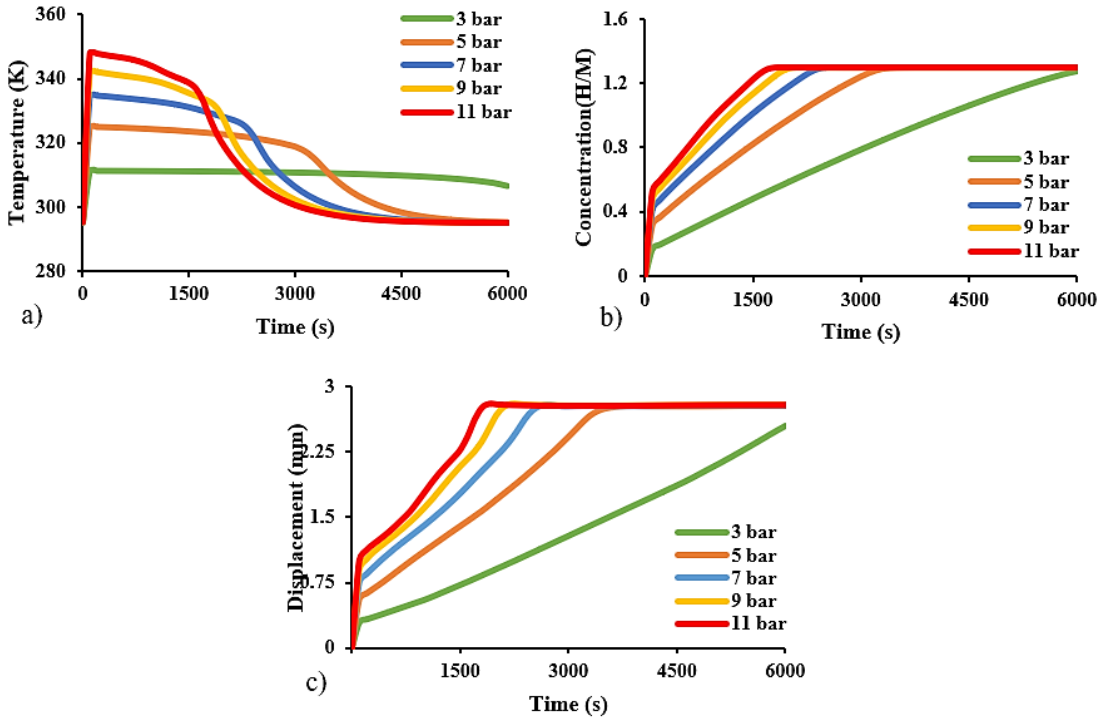

Figure 9: Effect of H_2 supply pressure on a) Average bed temperature b) Bed concentration c) Actuator displacement during hydriding process in composite bed (T_o =295K, P_o =3-11 bar, h=22W/m^{2}K, Bed thickness= 3 mm, Axial Pitch= 36mm, Spring constant= 7.874, Coils = 5($LaNi_5$) 8.32 ($LaNi_5$-Si))

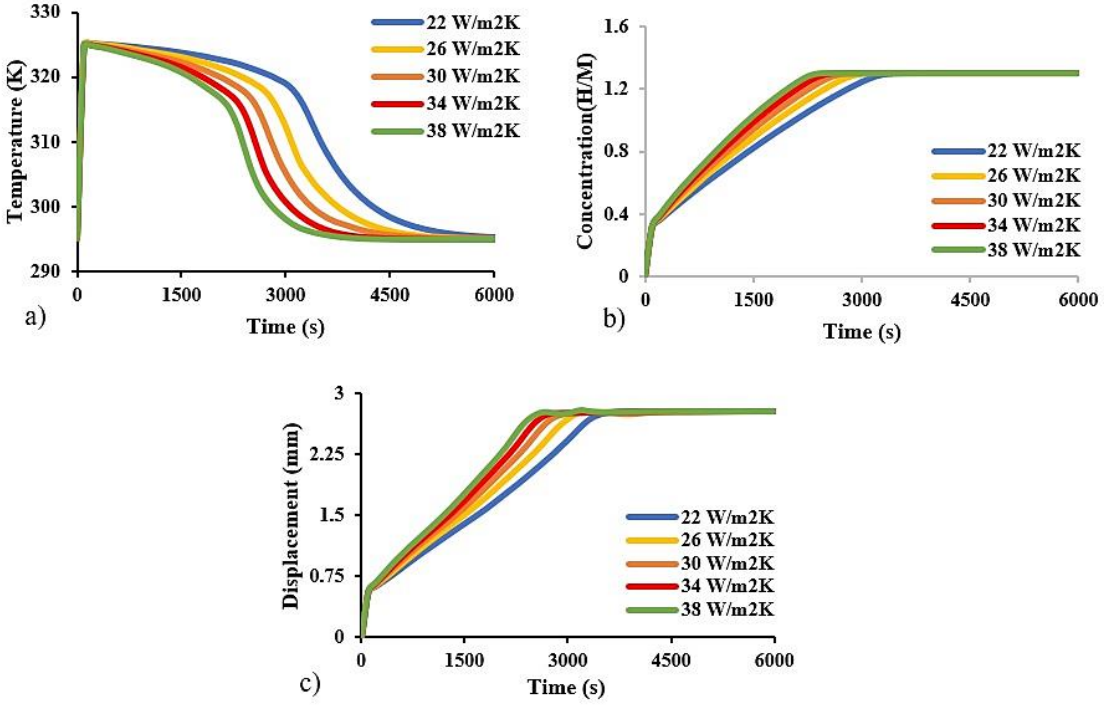

Figure 10: Effect of heat transfer coefficient on a) Average bed temperature b) Bed concentration c) Actuator displacement during hydriding process in composite bed (T_o =295K, P_o =5 bar, h=22-38W/m^{2}K, Bed thickness= 3 mm, Axial Pitch= 36mm, Spring constant= 7.874, Coils = 5($LaNi_5$) 8.32 ($LaNi_5$-Si))

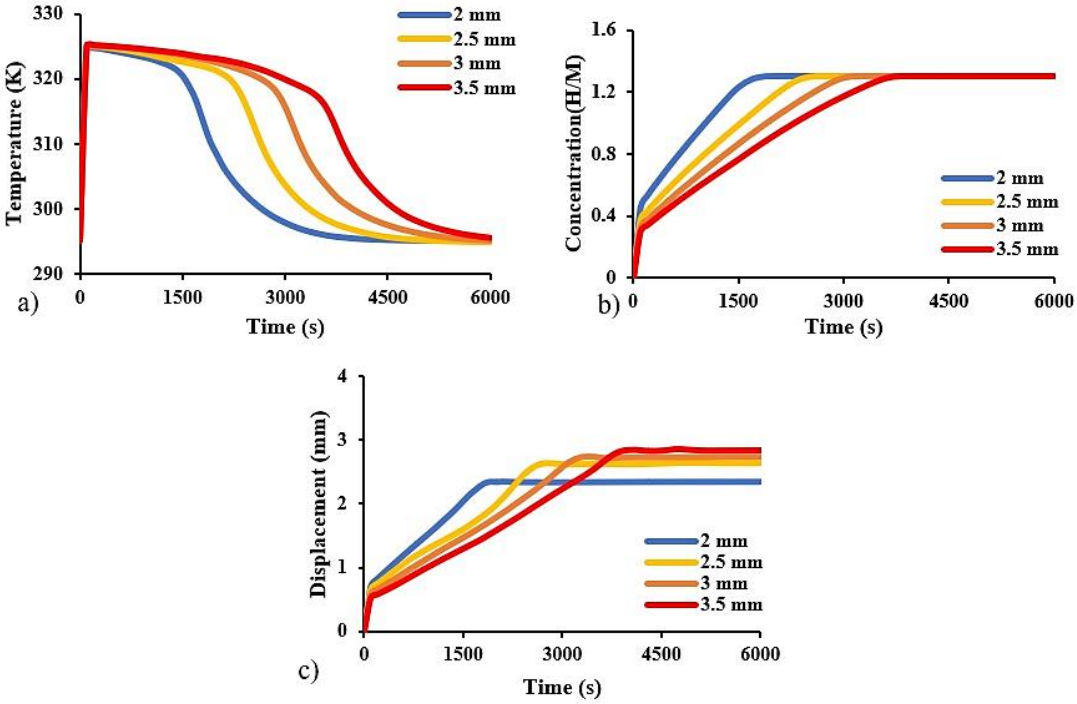

Figure 11: Effect of bed thickness on a) Average bed temperature b) Bed concentration c) Actuator displacement during hydriding process in composite bed (T_o =295K, P_o =5 bar, h=22-38W/m^{2}K, Bed thickness= 2-3.5 mm, Axial Pitch= 36mm, Spring constant= 7.874, Coils = 5($LaNi_5$) 8.32 ($LaNi_5$-Si))

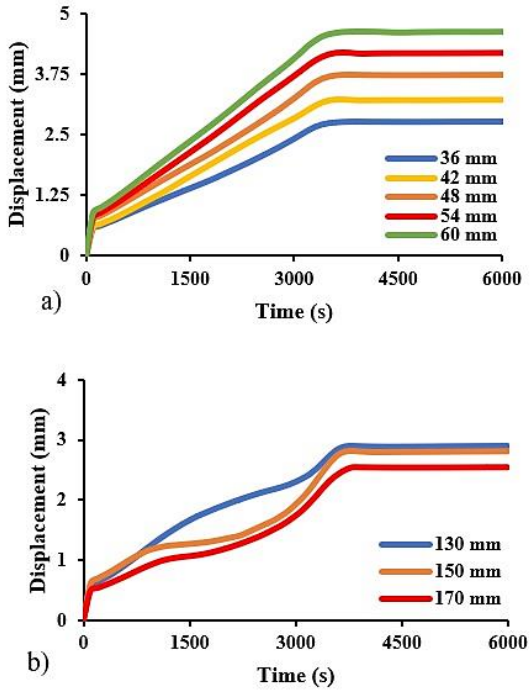

Figure 12: Effect of a) coil pitch and b) coil diameter on actuator displacement during hydriding process in granular bed (T_o =295K, P_o =5 bar, h=22W/m^{2}K, Bed thickness= 3 mm, Axial Pitch= 36-60 mm, Spring constant= 10.236-16.535, Coils = 5($LaNi_5$) 8.32 ($LaNi_5$-Si))